High-Sensitivity and Low-Hysteresis Inter-digital Type Capacitive Humidity Sensor on Glass Substrate by Aerosol Deposited $BaTiO_3$

*E. S. Kim, **Z. J. Wang, ***C. Wang, ****Z. Yao,
****J. G. Liang, *****N. Y. Kim

RFIC Center, Dept. of Electronic, Kwangwoon University, Seoul, South Korea
*esk@kw.ac.kr, **erikson@foxmail.com, ***kevin_wang@kw.ac.kr, ****yao9074@hotmail.com,
*****liangjun1991@hotmail.com, *****nykim@kw.ac.kr

ABSTRACT

Aerosol deposition (AD) is a shock-loading solidification ceramic film preparation technique exhibiting the advantages of room-temperature operation and highly efficient in film growth. Hygorscopic film which has a super mesoporous structure exhibits high sensitivies and fast response in humidity sensing. Our objective is to verify the feasibility of using AD by depositing $BaTiO_3$ films on a glass substrate with a Pt interdigital capacitor. Humidity sensing performances were evaluated by 400°C annealing temperature and 0.1-10 μm thickness of $BaTiO_3$. Films treatment in the thickness of 1.5 μm achieved excellent sensitivies in 178.6 ± 7.3 pF/%RH respectively. The surface hydrophilicity, pore volume, and open-pore ratio were analyzed as critical factors of the thickness related humidity sensing effects, and physical modeling exhibited an expanded humidity detection range, enhanced water vapor adsorption and desorption, and improved sensitivity to humidity.

Keywords: aerosol deposition (AD), humidity sensor, sensitivity, thickness effect, post-annelaing

1 INTRODUCTION

Aerosol deposition (AD) is a newly developed ceramic film preparation technique in which the film is grown by injecting high-speed (150–500 m/s) ceramic particles onto a substrate [1,2]. Humidity-sensing films are the core component of humidity sensors, exhibiting well-reproducible and regular variations of permittivity and conductivity in response to ambient humidity changes. Since AD film-growth is based on particle fragmentation and mutual bonding, macroscopic defects and internal pores will be generated during the deposition process. Limitations of this method include weak particle-to-particle bonds and surface pinholes, which can cause leakage currents and unstable dielectric properties and impair the electrical performance of the films [3,4,5]. However, these limitations become advantages in the field of humidity sensing wherein a mesoporous inner structure and a high-roughness surface can enhance the moisture absorption and desorption properties [6,7]. In this study, we investigated various thicknesses of AD-prepared $BaTiO_3$ films to determine the effects of thickness on the humidity-sensing properties.

Seven sensors with thicknesses from 0.1–10.0 μm were fabricated. To enhance the recrystallization of the $BaTiO_3$ grains, each sensor underwent a 400 °C thermal treatment for 2 h. The internal microstructure and surface morphology of the sensors were then evaluated and correlated with their corresponding humidity sensitivity and response/recovery properties. To further improve their sensing performance, the deposited films were post-annealed at different temperatures, and their grain growth state, crystal lattice, internal microstructure, and surface morphology were characterized in detail to model surface morphology variation at different treatment temperatures. Physical models for hygroscopic films with different cross-sectional density-distributions were constructed to explore the association between the physical structures and humidity sensing properties. Our study demonstrates the potential of the AD technique in hygroscopic film preparation, specifically with respect to optimizing the thickness of films for ultra-sensitive humidity sensing.

2 EXPERIMENTAL SECTION

2.1 AD Sensor Fabrication

Helium gas was used to accelerate the BaTiO3 aerosol during the AD process in order to increase the gas flow rate and particle impact velocity. The inner chamber gas flow rate was maintained at 3–8 L/min at an interior pressure of 1–7 Torr, and high-speed BaTiO3 particles were deposited on the glass substrate with a scanning speed of 1–2 mm/min. Table 1 lists the parameters, including the size of the nozzle orifice, distance between the nozzle and substrate, and operation time, that were applied to produce final deposited thicknesses from 0.1–10 μm. The fabricated sensors underwent post-annealing at a temperature of 400 °C for 2h, wherein the furnace temperature was raised and lowered by 5 °C/min.

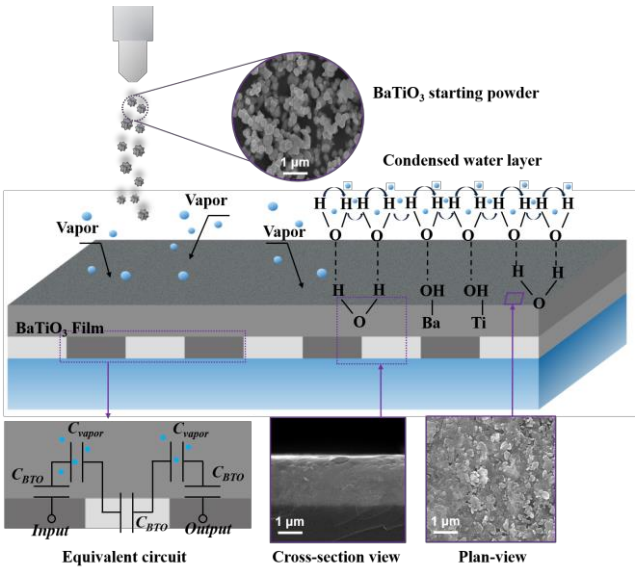

Fig. 1. AD hygroscoic film fabrication and humidity [13].

Table 1. AD and post-annealing treatment conditions detection [13].

Starting powder	$BaTiO_3$: 450 nm
Substrate	Glass
Size of nozzle orifice	10 × 0.4 mm^2
Scanning speed	1–2 mm/s
Working pressure	1–7 Torr
Carrier gas	He
Consumption of carrier gas	3–8 L/min
Distance between substrate and nozzle	5–10 mm
Deposition temperature	Room temperature
Deposition time	10–30 min
Deposition area	4.6 × 5.5 mm^2
Post-annealing temperature	400 °C
Post-annealing time	2 h
Environmental gas (post-annealing)	Atmosphere

2.2 Humidity Measurement

The hygroscopic film was prepared by employing AD on a glass substrate with interdigital capacitor electrodes (Fig. 1). Due to the naturally generated mesoporous microstructure and surface micro-holes, moisture can could easily penetrate the BaTiO3 film and condense to form chemical and physical water layers. This will cause the dielectric constant of the BaTiO3-water composite to increase and result in an increase of the capacitance, which can be detected using an inductance-capacitance-resistance meter (LCR meter) (IM3536, HIOKI E. E. Corp., Japan).

The measurement frequency of the LCR meter was set to 100 Hz, which is suitable for measuring the actual capacitance of the material [8]. The applied voltage was fixed at 1 V, and the ambient temperature was kept held at 23 °C. The sensors were tested in a humidity chamber (PDL-3J, ESPEC Corp., Japan) under ambient relative humidity (RH), which ranged from 20–90%. The response and recovery time was measured by a sudden humidity change from/to the ambient humidity in the measurement room (30% RH) to/from 90% RH, respectively. The sensitivity (s), which is a representative parameter employed to characterize the humidity-sensing property, was calculated using the following equation:

$$S = \frac{\Delta C}{\Delta RH}. \quad (1)$$

where $\triangle$ C is the capacitance change over the whole detection range (20-−90% RH) and $\triangle$RH is the value of ambient RH change from the lowest to the highest (90-20).

3 RESULTS AND DISCUSSION

3.1 Section and Sub-Section Headings

In Fig. 2, it can be seen that the film side view exhibits a specific transitional-density structure in which the density was the highest in the bottom region and decreased gradually to the top layer. A Fourier transformation graphs shows a focused low-frequency spectral power in the bottom layer (Fig. 2 (dii)) and more high-frequency power in the top layer (Fig. 2 (bii)), which indicates a dense and homogeneous grain distribution in the bottom section and a disordered grain distribution and more voids in the top layer. This cross-sectional transitional-density structure was caused by the different levels of the accumulated hammering effect at different film depths. The grains in the bottom layer experienced a more substantial hammering effect, which resulted in a denser grain arrangement. However, the top section experienced relatively fewer impacts, therefore many voids and large-sized irregular grains were distributed in the top region of film (Fig. 2 (bi)) when compared with the center (Fig. 2 (ci)) and bottom layers (Fig. 2 (di)).

3.2 Modeling the AD-Prepared Humidity-Sensing Film

The density of the AD film was high in the bottom layer where there were densely arranged grains and low in the top layer where there was high porosity. Based on these characteristics, we hypothesize that this specific cross-sectional structure is the reason for: (1) the expanded humidity detection range, (2) enhanced water vapor adsorption and desorption, and (3) improved humidity-sensing sensitivity [9]. To confirm this, we constructed models of three hygroscopic films with equal pore volumes but different cross-sectional density-distributions and investigated their humidity-sensing properties (Fig. 3) [10].

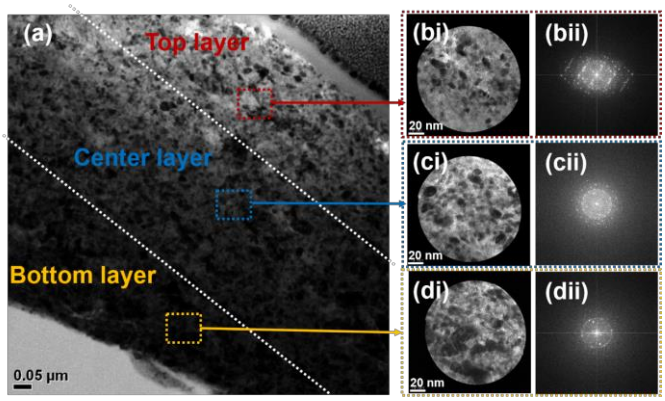

Fig. 2. TEM characterization of the cross-sectional transitional-density structure, (bi) – (di) partially enlarged views of the different layers, and (bii) – (dii) their Fourier transforms [13].

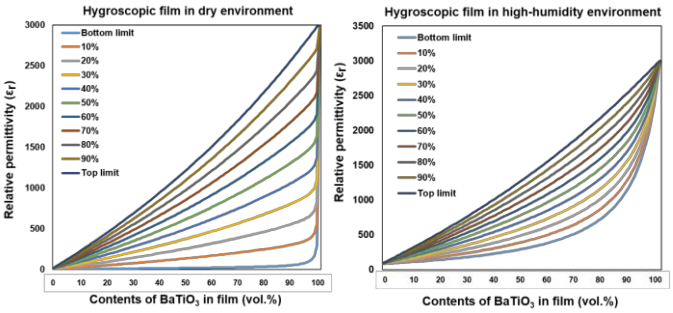

(a) (b)

Fig. 4. Modeling and sensitivity predication of hygroscopic films with different cross-sectional density distributions: (a) relative permittivity change vs the $BaTiO_3$ content and the connected ratio in a dry environment, in (b) a high-humidity environment [13].

3.3 Improved Humidity-Sensing Sensitivity

Hygroscopic films in a humid environment can be regarded as a composite structure consisting of condensed water and $BaTiO_3$ grains, and the dielectric constant of water ${}^{\varepsilon}H_2O$ in this case is defined as [11]

$$\varepsilon_{H_2O} = 78[1 - 4.6 \times 10^{-4}(T - 298) + 8.8 \times 10^{-6}(T - 298)^2] \quad (2)$$

where T is the absolute temperature. Since our measurements were performed at room temperature (23 °C), ${}^{\varepsilon}H_2O$ was calculated to be 78.54. In these models, the film was approximated as a triple-layer structure with different density layers in which the relative permittivity of each layer (ε_T, ε_C, ε_B) varied but could be estimated based on the fractional volume of $BaTiO_3$ using the Hashin–Shtrikman bounds [12]. The relative permittivity of the hygroscopic film in a dry and high-humidity environment, depending on the $BaTiO_3$ grain connected fraction (%) and the top and bottom limits, were calculated using Eqs. 3 and 4 and are plotted in Figs. 4 (a) and (b).

$$\varepsilon_{Top} = \varepsilon_{BTO}V_{BTO} + \varepsilon_{Air}V_{Air} - \frac{V_{BTO}V_{Air}(\varepsilon_{BTO}-\varepsilon_{Air})^2}{\varepsilon_{BTO}V_{Air}+\varepsilon_{Air}V_{BTO}+(d-1)\varepsilon_{BTO}} \quad (3)$$

$$\varepsilon_{Bottom} = \varepsilon_{BTO}V_{BTO} + \varepsilon_{Air}V_{Air} - \frac{V_{BTO}V_{Air}(\varepsilon_{BTO}-\varepsilon_{Air})^2}{\varepsilon_{BTO}V_{Air}+\varepsilon_{Air}V_{BTO}+(d-1)\varepsilon_{Air}} \quad (4)$$

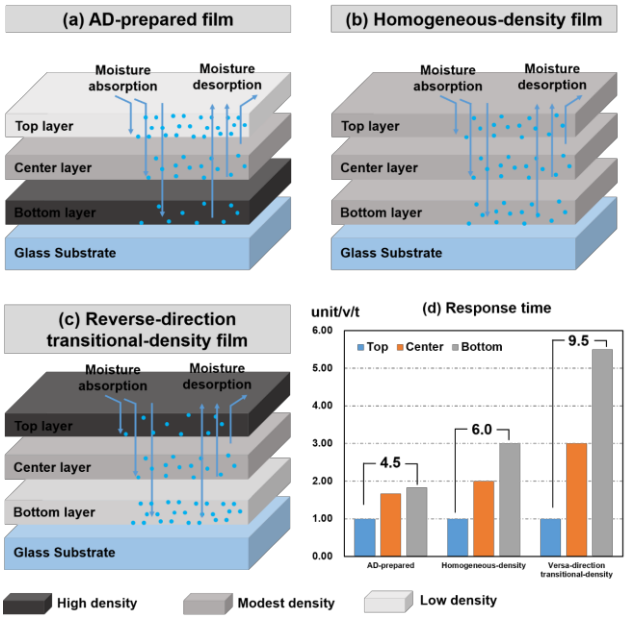

Fig. 3. Comparison of the models of three types of hygroscopic film with different cross-sectional density distributions. (a) AD-prepared film with a transitional density wherein the bottom layer has the highest density. (b) Homogeneous-density film. (c) Reverse direction transitional density film wherein the top layer has the highest density. (d) Response time prediction for the three models [13].

The results of the current study confirmed that films with a high moisture permeability can be prepared using the AD method. When the thickness is optimal, they then exhibit an increased surface hydrophilicity, pore volume, and open-pore ratio, along with a more advantageous inner mesoporous microstructure.

4 CONCLUSION

In this study, $BaTiO_3$ film thicknesses ranging from 0.1–10.0 μm were prepared in order to test the feasibility of AD on the preparation of the ultra-sensitive hygroscopic film and the effects of thickness on the humidity-sensing properties. We found the AD-prepared $BaTiO_3$ hygroscopic film exhibited a transitional-density cross structure that appeared to expand the detection limits, promote moisture absorption and desorption, and improve the humidity sensitivity. With the advantages of a low thermal energy cost, straightforward operation, ability to store the raw materials long-term, and ultra-sensitive properties of the film, the AD technique holds promise for the preparation of hygroscopic film in production at an industrial scale.

5 ACKNOWLEGEMENTS

This work was supported by a National Research Foundation of Korea (NRF) grant funded by the Korea government (MSIP; Ministry of Science, ICT, & Future Planning) (Nos. 2011-0030079 and 2017R1C1B5017013) and a grant from the Korean government (MEST) (Nos. 2015R1D1A1A09057081 and 2016K000117) by funded by the Commercializations Promotion Agency for R&D Outcomes. This work was also supported by a Research Grant from Kwangwoon University in 2018.

6 REFERENCES

[1] J. Akedo, J. Therm. Spray Technol. Vol. 17, 181–198, 2008.
[2] D. Hanft, J. Exner, M. Schubert, T. Stocker, P. Fuierer, R. Moos, J. Ceram. Sci. Technol. Vol. 6, 147–181, 2015.
[3] M. Oh, S.M. Nam, Thin Solid Films. Vol. 518, 6531–6536, 2010.
[4] J.-M. Oh, S.-M. Nam, Jpn. J. Appl. Phys. Vol. 48, 2009.
[5] H.-K. Kim, J.-M. Oh, S. In Kim, H.-J. Kim, C. Lee, S.-M. Nam, Nanoscale Res. Lett. Vol. 7, 2012.
[6] Z. Yao, C. Wang, Y. Li, H.-K. Kim, N.-Y. Kim, Nanoscale Res. Lett. Vol. 9, 435, 2014.
[7] C. Wang, H.J. Kim, F.Y. Meng, H.K. Kim, Y. Li, Z. Yao, N.Y. Kim, IEEE Electron Device Lett. Vol. 37, 220–223, 2016.
[8] A. Tripathy, S. Pramanik, A. Manna, S. Bhuyan, N. Azrin Shah, Z. Radzi, N. Abu Osman, Sensors. Vol. 16, 1135, 2016.
[9] H. Farahani, R. Wagiran, M.N. Hamidon, Humidity sensors principle, mechanism, and fabrication technologies: A comprehensive review, 2014.
[10] J.M. Oh, N.H. Kim, S.C. Choi, S.M. Nam, Mater. Sci. Eng. B. Vol. 161, 80–84, 2009.
[11] J. Wang, G. Song, Thin Solid Films. Vol. 515, 8776–8779, 2007.
[12] Y.C. Yeh, T.Y. Tseng, J. Mater. Sci. Vol. 24, 2739–2745, 1989.
[13] J.G. Liang, E. S. Kim, C. Wang, M. Y. Cho, J. M. Oh, N. Y. Kim, Sensors and Actuators B: Chemical. Vol. 265, 632-643, 2018.